

# Diphenylalanine as a Reductionist Model for the Mechanistic Characterization of $\beta$ -Amyloid Modulators

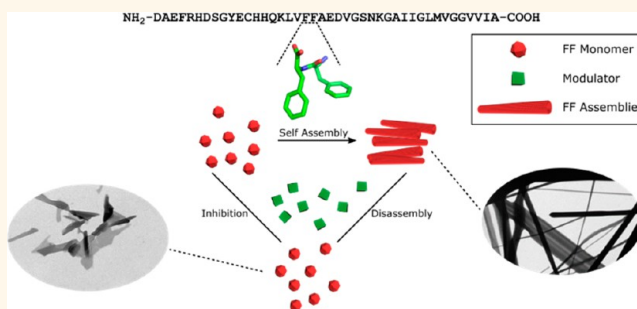
Sayanti Brahmachari,<sup>†</sup> Zohar A. Arnon,<sup>†</sup> Anat Frydman-Marom,<sup>†</sup> Ehud Gazit,<sup>\*,†,‡</sup> and Lihi Adler-Abramovich<sup>\*,§</sup>

<sup>†</sup>Department of Molecular Microbiology and Biotechnology, <sup>‡</sup>Department of Materials Science and Engineering, Iby and Aladar Fleischman Faculty of Engineering, and <sup>§</sup>Department of Oral Biology, The Goldschleger School of Dental Medicine, Sackler Faculty of Medicine, Tel Aviv University, Ramat Aviv, Tel Aviv 69978, Israel

## S Supporting Information

**ABSTRACT:** The phenomenon of protein aggregation into amyloid fibrils is associated with a large number of major diseases of unrelated etiology. Unraveling the mechanism of amyloid self-assembly and identifying therapeutic directions to control this process are of utmost importance. Research in this field has been hampered by several challenges, including reproducibility, low protein purification yields, and the inherent aggregation propensity of amyloidogenic proteins, making them extremely difficult to study. Herein, on the basis of the similarity in the assembly mechanism, as well as the physical, chemical, and biological characteristics, of diphenylalanine nanostructures and aromatic amino acid containing amyloid fibrils, we report a simple, yet robust peptide-based platform that could be used for screening of small molecules potentially capable of interfering with the aggregation process and for mechanistic exploration of their mode of action. The system was validated using four small-molecule inhibitors, and the effect was examined *via* turbidity assay, thioflavin T fluorescence, and electron microscopy. The aggregation profile of diphenylalanine was very similar to that of  $\beta$ -amyloid polypeptide in the presence of the modulators. Rosmarinic acid emerged as an extremely potent inhibitor and a destabilizer of the aggregates. The effect of stoichiometric variation of rosmarinic acid on the process of destabilization was also probed using a microfluidic technique. Finally, the formation of equimolar complexes of diphenylalanine and inhibitors was detected using mass spectrometry. This approach not only provides a system for high-throughput screening of possible inhibitor molecules from larger libraries of modulators, but is also highly useful for understanding the mechanistic aspects of the interactions leading to the process of inhibition.

**KEYWORDS:** diphenylalanine, high-throughput screening, amyloids, inhibitors, microfluidics, mass spectrometry



Various amyloid diseases of unrelated etiologies, including Alzheimer's disease, Parkinson's disease, amyotrophic lateral sclerosis, Huntington's disease, Creutzfeldt-Jakob disease, and type II diabetes, are associated with noncovalent interactions between peptides or proteins leading to their aggregation.<sup>1–5</sup> These disorders are typically characterized by the accumulation of disease-specific proteins or peptides into  $\beta$ -sheet rich plaques.<sup>6</sup> Over the years, continuous efforts have been made to examine the molecular basis of such associations, their mechanism of progression, and the ways to prevent these processes.<sup>3,7–14</sup> The common aggregation pattern of a variety of unrelated proteins has prompted the search for common mechanisms of progression and treatment for most of these diseases. This putative generic mechanism of action was supported when polyphenols were

found to be effective in reducing the aggregation of several amyloidogenic proteins of unrelated origin.<sup>15–18</sup> Several in-depth investigations have revealed the cumulative role of hydrogen bonding, hydrophobic interactions, and steric interactions in the formation of these aggregates.<sup>19–21</sup> While aliphatic amyloidogenic peptides are known, the interactions between aromatic moieties often play a central role in facilitating molecular recognition leading to enhanced aggregation. Although aromatic amino acids are conserved in nature, their predominant presence in the structural backbone of aggregative proteins is of particular interest.<sup>10,16</sup> Aromatic

Received: March 12, 2017

Accepted: June 2, 2017

Published: June 2, 2017

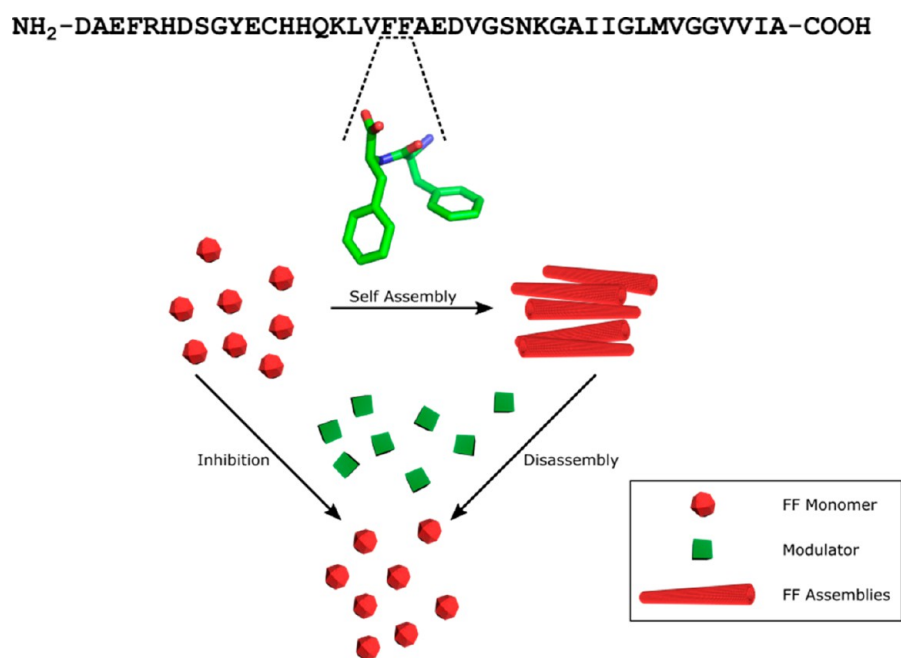


**Figure 1.** Diagram representing the similarity of the FF dipeptide and the  $\beta$ -amyloid polypeptide and the use of FF as a model system for screening of potential modulators.

moieties often increase the aggregation tendency of a protein and play a major role in stabilizing the formed aggregates of very short peptides.<sup>21</sup> A global analysis of the aggregation propensity of all natural amino acids proposed that tryptophan and phenylalanine are considerably more amyloidogenic than the aliphatic amino acids.<sup>10</sup>

However, the intrinsic aggregation tendency of the proteins themselves makes structure-based studies extremely challenging.<sup>22</sup> *In vitro* studies generally necessitate the tedious isolation and purification of the proteins with high yield. The slow and laborious isolation process of these aggregation-prone proteins for biophysical analyses using spectroscopic or microscopic techniques sometimes leads to false positive results.<sup>23</sup> Often, working with full-length proteins leads to many variations and low reproducibility of the results.<sup>24</sup> Hence, establishing an alternative, easy to handle, platform that does not involve the challenge of protein purification and simultaneously gives reproducible results is of utmost importance.

To this end, we chose a reductionist approach aimed at understanding the key factors that trigger the cascade of protein aggregation.<sup>25–28</sup> Previous studies have demonstrated the ability of short penta- and heptapeptides to aggregate into amyloid-like structures showing biophysical properties similar to larger polypeptides.<sup>4,29</sup> Systematic investigation of  $\beta$ -amyloid polypeptide ( $A\beta$ ) led to identification of the diphenylalanine (FF) dipeptide, which was shown to form nanotubes highly resembling the characteristic amyloid fibrils.<sup>30,31</sup> The FF dipeptide was identified as the smallest unit or the core recognition motif of  $\beta$ -amyloid polypeptide that undergoes self-assembly into ordered structures (Figure 1). The exchange of phenylalanine residues at the C-terminus of  $A\beta$  (1–42) with hydrophobic residues leads to a slower aggregation rate, while increasing the number of phenylalanine residues leads to higher aggregation propensities.<sup>32</sup> Spectroscopic investigations also indicated a  $\beta$ -sheet-like organization of the FF assemblies.<sup>30</sup> Moreover, most of the familial mutations within the polypeptide translated region leading to the early onset of

Alzheimer's disease, such as Iowa, Arctic, Dutch, Italian, Ottawa, and Flemish mutations, are located adjacent to the FF region.<sup>33</sup> We therefore believe that the two phenylalanine residues in the 19 and 20 positions of the  $A\beta$  polypeptide play a significant role in the initial steps of interaction leading to the formation of the plaques. Furthermore, NMR studies have demonstrated the specific binding of inhibitory agents to the FF region of the full-length polypeptide.<sup>25,34</sup> The FF region thus represents both a key molecular recognition and self-assembly unit, as well as a validated drug target for efficient inhibition of the amyloidogenic process. Recently it was also shown that similar to amyloidogenic polypeptides<sup>35</sup> FF ultrastructure formation is accompanied by the formation of reactive oxygen species,<sup>36</sup> thus supporting the functional similarity of the short peptide assemblies and the native amyloids (Table 1). Additionally, the similarity in the photoluminescence properties of the FF module<sup>37</sup> and several aggregative polypeptides,<sup>38,39</sup> as well as their similar mechanical properties,<sup>40–42</sup> is indicative of a common generic form of noncovalent packing. The pivotal

**Table 1. Highlighting the Similarities between the Amyloidogenic Peptides and the Dipeptide**

properties	amyloidogenic proteins	diphenylalanine
assembly	weeks–days	immediate
secondary structure	$\beta$ -sheet structure	$\beta$ -sheet structure
molecular weight	>4000 g/mol	312 g/mol
photoluminescence	autofluorescence	autofluorescence
cross-polarized light	birefringence with Congo Red	birefringence with Congo Red
spectral binding	binds to ThT	binds to ThT
thermal stability [°C]	≥130	≥150
mechanical strength [Gpa]	3.3 ± 0.4	~19
reactive oxygen species	produces ROS	produces ROS
modulators	rosmarinic acid, NDGA, tetracycline, EGCG	rosmarinic acid, NDGA, tetracycline, EGCG

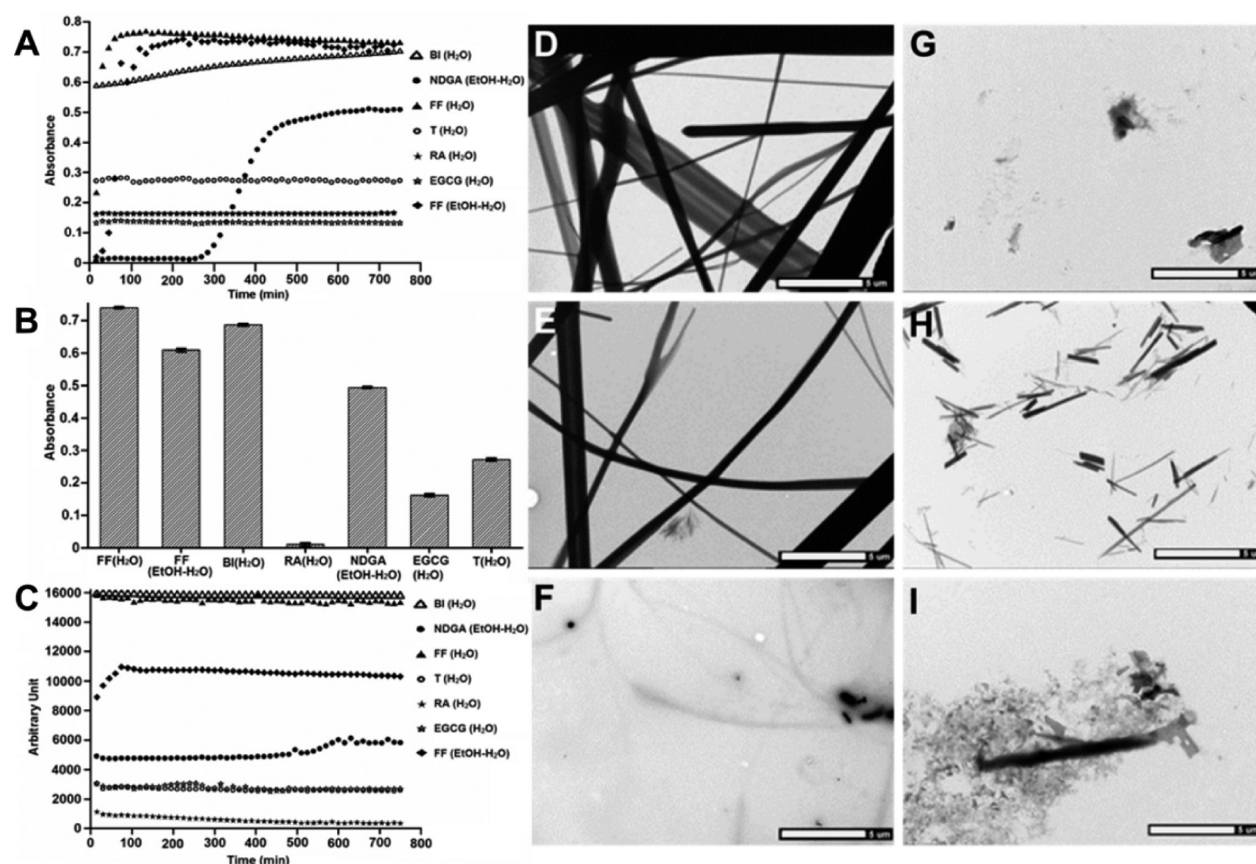


Figure 2. (A) Turbidity measured at 405 nm over 12 h for 6.4 mM FF in the presence of 6.4 mM modulators. (B) End point turbidity measured at 405 nm after 48 h incubation of 6.4 mM FF with 5 mM of modulators. (C) Fluorescence emission intensity of 100 mM ThT measured at 490 nm recorded over 12 h of incubation with 24 mM FF and 6.4 mM modulators. (D) TEM image of FF nanotubes. (E) FF nanotubes with BI. (F) FF nanotubes with RA. (G) FF nanotubes with tetracycline. (H) FF nanotubes with NDGA. (I) FF nanotubes with EGCG. (The scale bar denotes 5  $\mu$ m.)

importance of the FF motif is also reflected in the identification of metalloproteases found in *E. coli* and other bacteria, which specifically target the FF motif.<sup>43</sup> This enzyme appears to allow the growth of bacteria under conditions that promote protein unfolding. Thus, FF could be used as a model for amyloid systems, as it is endowed with most of the characteristics of amyloid-forming proteins.

Here, we aimed at designing an amyloid modulator screening model system using the FF peptide. One of the common strategies adopted in the search for a cure for these diseases is to identify small drug-like molecular entities capable of interfering with the process of self-aggregation, including small molecules and peptides.<sup>44–48</sup> Among them, a set of polyphenol-based inhibitors, which were previously identified as  $\beta$ -amyloid modulators,<sup>16,17</sup> was selected for the validation of the model system. The inhibition pattern of FF aggregation by the polyphenols was studied using a turbidity assay, a thioflavin T (ThT) fluorescence assay, and electron microscopy analysis. Microfluidics was employed to gain further insight into the process of disassembly, and mass spectrometry analysis was used to reveal interactions taking place between FF and the amyloid modulators. From the list of selected inhibitors, rosmarinic acid (RA) was found to be an extremely potent inhibitor of FF aggregation both before and after the crucial nucleation. The mechanism of inhibition by RA was further studied in detail using microfluidic techniques. Although some *in vitro* screening systems have been previously reported,<sup>7,22</sup>

this is a study primarily involving the utilization of a simple dipeptide system instead of a complex polypeptide or a full-length protein, thus providing the advantage of inexpensive materials, as well as a facile and short fibril formation process, thereby allowing high-throughput screening for possible small-molecular amyloid modulators. The generality of the developed platform will enable the identification of potential drug modalities that might be simultaneously effective toward more than one amyloid disease.

## RESULTS AND DISCUSSION

**The Amyloid Modulators Library.** A set of four molecules previously shown to inhibit and disassemble the ordered structures formed by different amyloidogenic peptides was selected for this analysis: RA, nordihydroguaiaretic acid (NDGA), tetracycline, and epigallocatechin gallate (EGCG). RA, an active ingredient of some culinary herbs, such as rosemary, basil, and sage, significantly reduces the cytotoxicity of  $A\beta$ -oligomers in cultured rat pheochromocytoma (PC12) cells.<sup>49,50</sup> RA also acts as a peroxynitride scavenger and was shown to prevent memory impairments induced by  $A\beta_{25-35}$  injection in a mice model.<sup>50</sup> The polyphenolic antioxidant NDGA reduces the cytotoxicity of  $A\beta$ -fibrils toward cultured hippocampal neurons in a concentration-dependent manner.<sup>51,52</sup> The classical antibiotic tetracycline has also been reported to mitigate the toxic effect of  $A\beta$ -oligomers and to disassemble preformed oligomeric aggregates. Interestingly,

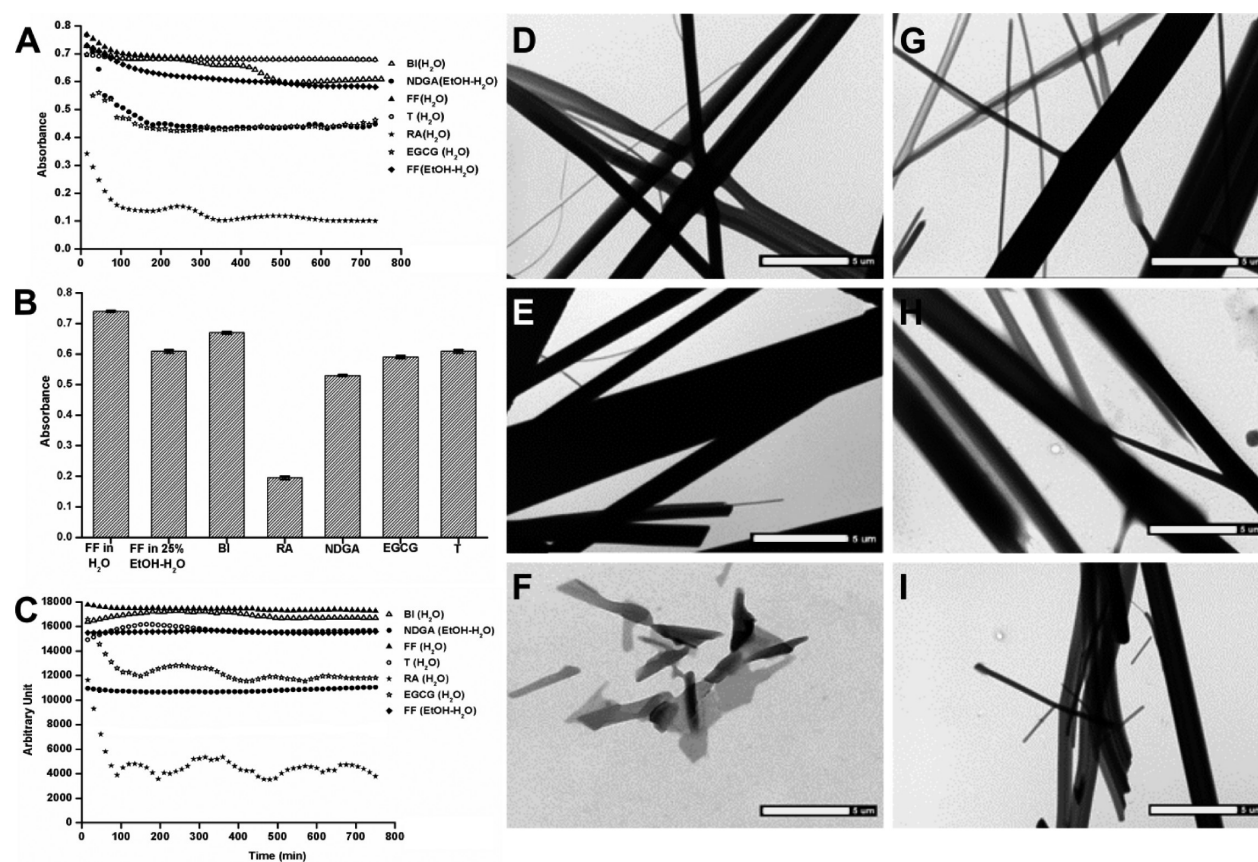


**Figure 3.** (A) Turbidity measured at 405 nm over 12 h for 6.4 mM preformed FF in the presence of 6.4 mM modulators. (B) End point turbidity measured at 405 nm after 48 h of incubation of 6.4 mM FF with 5 mM of modulators. (C) Fluorescence emission intensity of 100 mM ThT measured at 490 nm recorded over 12 h of incubation with 24 mM preformed FF in 24 mM modulators. (D) TEM image of FF nanotubes. (E) FF nanotubes with BI. (F) FF nanotubes with RA. (G) FF nanotubes with tetracycline. (H) FF nanotubes with NDGA. (I) FF nanotubes with EGCG. (The scale bar denotes 5 μm.)

tetracycline and its group of compounds have been reported to have a pronounced disassembling effect on several amyloidal proteins, including  $A\beta_{1-40}$  and  $A\beta_{1-42}$ , transthyretin,  $\beta_2$ -microglobulin, and Islet amyloid polypeptide (IAPP).<sup>9,53,54</sup> EGCG, a principal component of green tea, has been demonstrated to affect the aggregation pattern and cytotoxicity of aggregative proteins such as  $A\beta$  and  $\alpha$ -synuclein.<sup>15,55</sup> These modulators were also found to inhibit the aggregation process as well as destabilize preformed fibrils of  $A\beta_{1-40}$  and  $A\beta_{1-42}$ .<sup>9,18,51</sup> We also used benzimidazole (BI), which is commonly used as a probe for imaging proteins such as Tau and  $A\beta$ , as a negative control molecule. It has been established that BI does not interact with IAPP and has no effect on its aggregation.<sup>56</sup>

**Tuning the Assembly Process.** For studying the aggregation kinetics of the model FF peptide in the presence of the selected molecules, we performed a turbidity assay (Figure 2A). FF was added to individual stock solutions of the modulators at an equimolar ratio. The absorbance of the mixtures was recorded at 405 nm and plotted for 12 h. Interestingly, we observed very low growth of the assemblies when incubated with RA, tetracycline, or EGCG, whereas with NDGA, growth of nanostructures was observed after incubation for 5 h and the extent of growth was about 40% less than that observed in the control FF system without any modulator or in the presence of BI, which was similar to the control. To gain a distinct notion about the effect of each modulator on the

process of assembly over time, FF was added to modulator stocks and the turbidity was measured following 48 h of incubation (Figure 2B). The turbidity after 48 h showed an abundance of nanostructures in the presence of BI. However, formation of the nanostructures was significantly reduced in the presence of EGCG followed by tetracycline and NDGA, while almost no growth was observed in the presence of RA. Hence the order of growth inhibition ability is RA > EGCG > tetracycline > NDGA  $\gg$  BI.

To further validate the effect of the examined molecules on the aggregation process of FF, we used the ThT binding assay. We studied the formation kinetics of FF fibers in the presence of RA, EGCG, tetracycline, or BI. ThT was added to the modulator solutions followed by the addition of FF in HFIP. The rate of fibril genesis was monitored by recording the emission intensity of ThT at 490 nm over 12 h. The results were indeed quite similar to those of the turbidity assay. Predominant impedance in the formation rate of the structures was observed when FF was incubated with RA, tetracycline, and EGCG, about 50% growth of FF fibrils was observed following incubation with NDGA, whereas a near normal growth of the structures was observed in the presence of BI (Figure 2C).

In order to visualize the nanostructures formed by FF in the presence of the examined molecules, we subjected the systems to transmission electron microscopy (TEM) studies (Figure 2D–I). FF was added to the modulator stock solutions at an equimolar ratio and incubated for 24 h. The samples were

subsequently imaged using TEM. The TEM images of the control FF and BI clearly showed numerous fibers of varying diameters, while no fibers of similar nature were observed when FF was treated with RA, and only amorphous aggregates were identified (Figure 2D–F). When FF samples were incubated with NDGA, only very small fibers, as compared to the control, were detected (Figure 2G). Absolutely no fiber formation was noted when tetracycline or EGCG was used (Figure 2H,I).

Hence all the studied molecules exhibit a pronounced effect on the aggregation of the FF peptide. In the case of RA, the turbidity assay, end point analysis, and the ThT assay clearly show the lack of FF aggregation (Figure 2A), which is probably due to the interference of RA with the initial nucleation process of FF and its effect on the aggregation pathway of the system. While the TEM image (Figure 2F) does show some fibers, the morphology seems extremely different from the typical morphology of the FF nanotubes. Similarly, the turbidity assay, end point analysis, and the ThT assay of tetracycline and EGCG highlight the significant impedance in the self-aggregation of the FF system. Indeed, the electron microscopy images (Figure 2G,I) indicate that the process of inhibition is probably manifested by the formation of amorphous aggregates, different from the typical FF nanostructures. Most interestingly, in the ThT and turbidity assays of NDGA we can clearly observe a delayed initiation of the aggregation of FF. Moreover, with complete concurrence with these assays, the TEM image (Figure 2H) clearly shows the presence of small FF nanotubes instead of the longer ones. In addition, the lack of effect of BI on the aggregation of FF is observed in all experiments.

**Disassembly of Diphenylalanine by the Introduction of Modulators.** Next, we aimed to determine whether the modulators can also trigger a process of disassembly by analyzing their effect on preformed fibers using a turbidity assay (Figure 3A). FF structures were prepared, and after 2 h, RA, EGCG, NDGA, tetracycline, or BI stock solutions were added at an equimolar ratio and the absorbance of the mixtures at 405 nm was recorded over 12 h. Remarkably, a significant decrease in the turbidity was observed for the fibers incubated with RA, indicating degradation of the fibers, with almost 80% of the structures disassembled after 12 h. It was also noted that about 25% of the structures underwent disassembly following incubation with EGCG, but no further decay took place at this concentration ratio. Almost no disassembly was recorded when the structures were treated with NDGA, tetracycline, or BI after 12 h of incubation. We also recorded the effect of the treatment with modulators on preformed nanostructures after 48 h. Treatment with BI had no effect on the preformed fibrils, and treatment with tetracycline resulted in an almost negligible effect (Figure 3B). Remarkably, a significant effect was observed following incubation with RA, as almost 75% of the preformed fibrils disassembled after 48 h, while a slight effect of disassembly was observed after the treatment with EGCG and NDGA. Thus, the order of disassembling potential of the modulators is RA > EGCG > NDGA  $\gg$  tetracycline > BI.

Subsequently, we studied the effect of the molecules on preformed FF structures using the ThT binding assay. For this aim, FF structures were prepared and ThT was added. Following a 2 h incubation, solutions of RA, tetracycline, NDGA, EGCG, or BI were added in an equimolar ratio. The fluorescence intensity of ThT was recorded over 12 h. The results clearly indicated the potency of RA in disassembling the FF nanostructures, with an almost 90% decrease in fluorescence (Figure 3C). Similarly, an almost 25% decrease in fluorescence

intensity was observed following incubation with EGCG, while no significant disassembly was detected in the case of tetracycline, NDGA, or BI. Consistent with the results of the turbidity assay and TEM analysis, RA and EGCG emerge as potential inhibitors and destabilizers of FF fibrils.

Likewise, we aimed at understanding the process of disassembly of the preformed nanostructures upon treatment with the modulators using TEM. As before, FF structures were allowed to form over 2 h of incubation. Then, RA, tetracycline, EGCG, NDGA, or BI was added to the preformed nanostructures and further incubated for additional 24 h, and the samples were dried and imaged using TEM. The images obtained in the untreated sample and following treatment with BI showed the presence of intact FF fibers of about 10  $\mu\text{m}$  (Figure 3D,E). However, significantly scarcer fibers were observed after treatment with RA (Figure 3F). Although it was notable that fibers in the range of 10  $\mu\text{m}$  were abundant in the samples treated with NDGA, tetracycline, or EGCG, many broken small fibers in the range of 1  $\mu\text{m}$  or smaller were also observed in large numbers (Figure 3G–I).

Thus, analysis of the disassembling effect of the chosen set of modulators reveals that only RA can potentially disassemble the FF nanostructures. This is evident from the disassembly kinetics using the turbidity and the ThT assay, which demonstrate nice disassembly of the nanostructures over time (Figure 3A,C). These results are also supported by the TEM image (Figure 3F), where smaller nanostructures are observed, compared to the much larger ones in the control system (Figure 3D). Similarly, the turbidity and ThT assay of tetracycline and NDGA are in concurrence with the TEM images (Figure 3G,H), where almost unaffected FF nanotubes are abundantly observed. However, in the case of EGCG, although the turbidity assay, the end-point analysis, and the ThT assay show a reduction of the FF nanostructures, it is difficult to observe the same in the TEM images, probably due to its low effect. The turbidity assay, ThT assay, and the TEM images also validate BI as the control molecule, which does not affect the FF nanostructures.

**Direct Visualization of the Disassembly.** To gain further understanding of the disassembly process by RA and to visualize the process in real time, a microfluidic technique was applied. The use of microfluidics to monitor a single nanofiber in real time was recently described.<sup>57,58</sup> Initially, preformed FF nanotubes were injected into the microfluidic device and confined by micrometer-scale pillars of polydimethylsiloxane (PDMS). While the majority of assemblies were washed away from the device, a portion of the assemblies were restricted by the PDMS pillars and did not migrate upon the introduction of solution flow into the device. The microfluidic device has two inlets in which two different solutions can be injected at different flow rates. The two solutions are mixed into a homogeneous solution before flowing into the area of the confined structures. One solution consisted of 3.2 mM FF in 1% DMSO, while the other solution consisted of 3.2 mM FF and 1.4 mM RA. The flow rate ratio of the two solutions determines the ratio of RA:FF in the mixed solution. While the FF concentration in the mixed solution is permanently set to 3.2 mM, the RA concentration can vary from 0 to 1.4 mM with alteration of the flow rate ratio between the two solutions. We were therefore able to investigate the effectiveness of RA at various RA:FF ratios. When injecting only FF at the supercritical concentration of 3.2 mM, the structures rapidly elongated (Figure 4A).<sup>57</sup> When adding RA at an RA:FF ratio

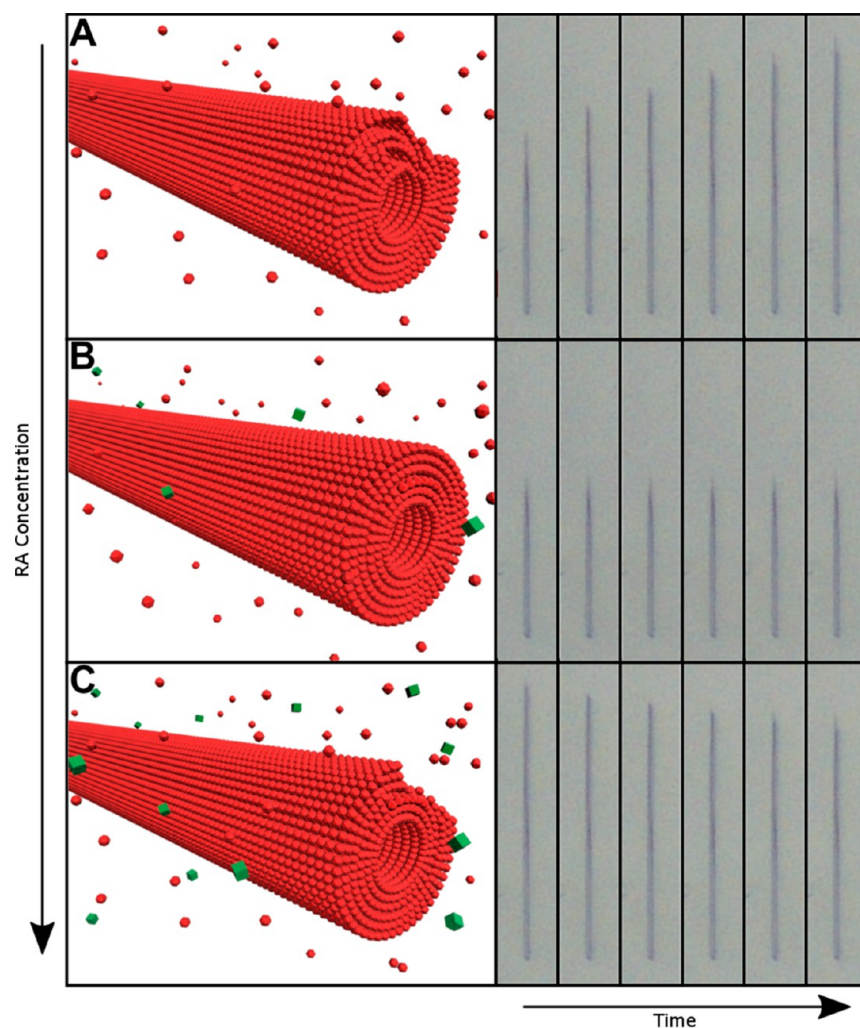


**Figure 4.** Illustration and imaging of FF nanotubes at varying concentration ratios of RA. (A) Elongation of the FF nanotubes in the absence of RA. (B) No elongation of the tubes at an RA:FF ratio of 0.18. (C) Degradation of the tubes at an RA:FF ratio of 0.36.

of 0.18, the assemblies no longer elongated and the length of the nanotubes remained the same (Figure 4B). Further increasing the RA:FF ratio to 0.36 resulted in disassembly of the structures and decrease in the nanotube length (Figure 4C). This visualization technique can clearly be used to show the impact and effectiveness of different compounds on self-assembly systems.

#### Probing the Interactions of FF and the Modulators.

Following the observed effect of the modulators on the assembly of FF, we were interested in studying the intermediate complexes and the nature of the interactions leading to the overall process of inhibition or disassembly.<sup>59</sup> Mass spectrometry has lately emerged as an important tool for studying the interplay of small molecules with amyloid-forming peptides and metaclusters.<sup>56,60,61</sup> Initially, we started with the study of FF in water using electron-spray-ionization mass spectrometry (Figure 5A). To detect the interactions between the peptide and the modulators, FF was dissolved in water, and all the examined modulators, as well as BI, were added in an equimolar ratio. We also studied the blank spectra of the modulators (Figures S1–S5, Supporting Information, SI). When FF was treated with BI, only the  $m/z$  of the FF monomer at 311 and of the FF dimer at 645 were observed (Figure 5B). However, in the presence of most modulators, the  $m/z$  corresponding to the

dimer completely vanished and only the signal of the monomer was observed. Following treatment with RA, in addition to the  $m/z$  peak at 311 corresponding to monomeric FF,  $m/z$  signals at 359, corresponding to blank RA, and at 671, corresponding to the FF–RA complex, were obtained (Figure 5C). Similarly, following treatment with either NDGA or EGCG, the major peak corresponded to the blank modulator followed by the monomeric FF and FF–modulator signals were observed (Figure 5D,F). However, for tetracycline the noted peaks corresponded to monomeric FF, blank tetracycline, and dimeric FF, while no signal for a FF–tetracycline heterodimer was obtained, which probably suggests the inhibition takes place *via* a route different from that of the other modulators (Figure 5E). While small peaks corresponding to modulator homodimers were obtained, the significantly higher intensity of the peaks corresponding to FF–modulator heterodimers suggests that the latter represent stable intermediate complexes. Moreover, the absence of such complexes in the case of BI and the significant decrease of dimeric FF in the presence of the modulators support the concept of strong interactions between FF and the modulators.

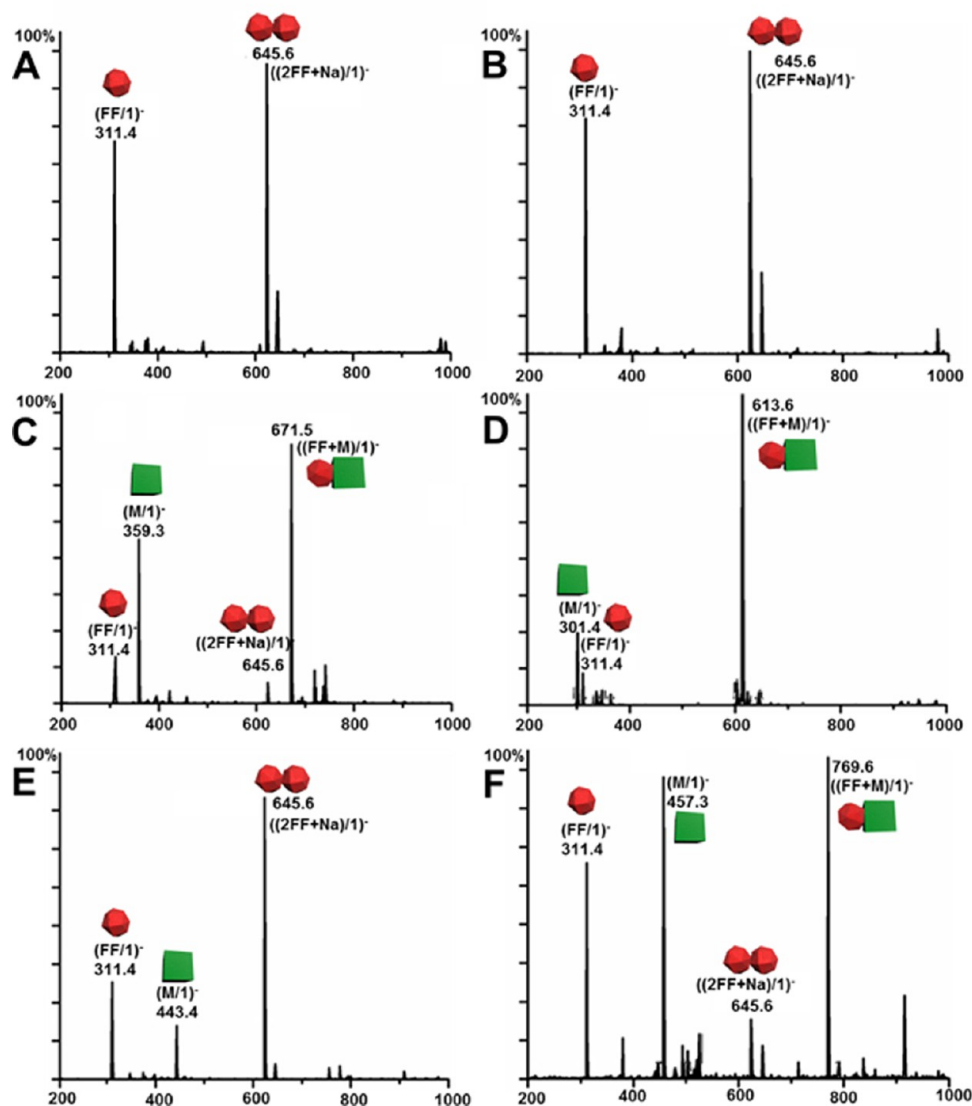


Figure 5. (A) FF, (B) FF with BI, (C) FF with RA, (D) FF with NDGA, (E) FF with tetracycline, and (F) FF with EGCG (M represents the modulators).

## CONCLUSIONS

Identifying small molecules that can modify the aggregation of various amyloid proteins and thus bearing the potential to serve as treatment for amyloid-related diseases has long been hampered by the lack of reliable screening systems. Here we present, as a proof of concept, a screening system based on the modulation of both the assembly and disassembly processes of FF assemblies. Our results demonstrate this platform to be inexpensive, reliable, reproducible, and easy to use, thus establishing a promising methodology for the identification of amyloid modulators. The extensive analysis of the modulation of FF assembly and disassembly by the four molecules examined here is in high accordance with their previously established effects on aromatic amino acid containing amyloidogenic proteins. Notably, the chosen molecules have different types of effects on amyloidogenic proteins, and the same specific patterns of interaction are reflected in our FF model system. Moreover, BI shows no effect on the genesis or disassembly of FF fibrils, as previously shown for IAPP.<sup>56</sup> The effect of RA on FF is quite analogous to its effect on  $A\beta$ , acting

as both a potent inhibitor and a destabilizer.<sup>9,18</sup> Similarly, EGCG, a known potential inhibitor and destabilizer of  $A\beta$  and  $\alpha$ -synuclein, displays a comparable effect on the FF system.<sup>15</sup> Likewise, tetracycline, which is known to be a strong inhibitor and weak destabilizer of  $A\beta$ ,<sup>53</sup> exerts a similar effect on the FF model system. Finally, the inhibition and destabilization effect of treatment with NDGA is similar to that observed in the case of  $A\beta$ .<sup>51</sup> This study establishes a system for high-throughput screening of possible inhibitor molecules of several amyloidogenic diseases, which is applicable for larger libraries of modulators.

## METHODS

**Materials.** The modulators (RA, tetracycline, NDGA, BI, and EGCG, purity  $\geq 98$ ), DMSO, thioflavin T, and hexafluoroisopropyl alcohol (HFIP) were procured from Sigma, and ultrapure water was obtained from Biological Industries. L-Diphenylalanine was purchased from Bachem at a purity level of  $>98\%$ .

**Preparation of Modulator Stock Solutions.** For most applications, stock solutions of the required concentration were prepared in 1% DMSO–water for RA, tetracycline, EGCG, and BI,

while NDGA was dissolved in 25% ethanol–water at room temperature. However, for TEM analysis 10% ethanol–water was used for preparing RA, tetracycline, EGCG, and BI solutions, while NDGA stock was prepared as described above.

**Turbidity Assay.** The modulator solutions were freshly prepared as described above to a concentration of 6.4 and 12.8 mM. For studying the process of assembly, FF was then dissolved in HFIP at a concentration of 320 mM and then added to the modulator solutions (6.4 mM) to achieve a concentration of 6.4 mM of FF. For the process of disassembly, a 12.8 mM FF in HFIP stock solution was prepared, and structures were formed. After 2 h the modulators (12.8 mM) were added and turbidity was recorded at 405 nm using an ELISA reader (Synergy HT, Biotek Instruments, Winooski, VT, USA). The final turbidity at 405 nm was also recorded after 48 h.

**ThT Fluorescence Emission Spectra.** Modulators were dissolved as described above to a concentration of 12.8 and 51.2 mM. In case of assembly, the FF (25.6 mM final concentration) was added to the solution of the modulator (12.8 mM final concentration), while for the disassembly, the modulators (final concentration of 25.6 mM) were added to preformed nanostructures (final concentration of 25.6 mM). ThT fluorescence emission at 490 nm (excitation at 450 nm) was collected *via* the BMG Labtech Clariostar plate reader for 12 h. For the process of assembly, ThT (100  $\mu$ M final concentration) was added to the solution of the modulators, while for the disassembly ThT was added to the preformed FF nanostructures.

**Transmission Electron Microscopy.** Modulators were prepared as described above at a concentration of 6.4 and 12.8 mM. For the process of assembly, FF in HFIP was added to the solution of modulators. In case of disassembly, the structures were allowed to form in solution followed by the addition of the modulators. The solutions were incubated for 24 h, and a 10  $\mu$ L aliquot was placed on 400-mesh copper grids. After 1 min, excess fluids were removed. Samples were viewed using a JEOL 1200EX electron microscope operating at 80 kV. Calculating the diameter of amyloid fibers of FF was performed by measuring five fibers from three different images.

**Microfluidic Experiments.** Microfluidic channels were fabricated in PDMS, using SU8 on silicon masters and standard soft lithography techniques. Inlets and outlets were punched, and PDMS was then plasma bonded to glass slides to create sealed devices. Preformed crystalline structures were inserted into the device. Then, a flow of solutions of known concentrations of monomeric FF and RA was injected at a rate of 4  $\mu$ L/h using Cetoni GmbH neMESYS syringe pumps (Korbussen, Germany). This process was examined under an OPTIKA XDS-2 Trinocular inverted microscope, and images were captured every 5 s. Captured images were analyzed using ImageJ 1.45S.

**Mass Spectrometry.** The samples were prepared for mass spectrometry by dissolving the modulators and FF, both at a concentration of 1 mM, in water by heating to 90 °C. Mass spectrometry was recorded using an Acquity UPLC system coupled to a TQD XEVO triple quadrupole ESI source mass spectrometer system from Waters (Milford, MA, USA).

## ASSOCIATED CONTENT

### Supporting Information

The Supporting Information is available free of charge on the ACS Publications website at DOI: 10.1021/acsnano.7b01662.

Mass spectrometry data of blank inhibitors (PDF)

## AUTHOR INFORMATION

### Corresponding Authors

\*E-mail (E. Gazit): [ehudg@post.tau.ac.il](mailto:ehudg@post.tau.ac.il).

\*E-mail (L. Adler-Abramovich): [LihiaA@tauex.tau.ac.il](mailto:LihiaA@tauex.tau.ac.il).

### ORCID

Sayanti Brahmachari: 0000-0002-5816-8805

### Notes

The authors declare no competing financial interest.

## ACKNOWLEDGMENTS

This work was supported in part by grants from the European Research Council (ERC) under the European Union's Horizon 2020 research and innovation program (grant agreement no. 694426) and Helmsley Charitable Trust for a Focal Technology Area on Nanomedicine for Personalized Therapeutics (E.G.). S.B. gratefully acknowledges the Centre for Nanoscience and Nanotechnology of Tel Aviv University and the Planning and Budget Committee, Israel, for financial support. The authors thank Dr. Sharon Gilead for helpful discussions, Dr. Luba Burlaka for TEM, Dr. Tal Noam for mass spectroscopy, Dr. Sigal Rencus-Lazar for language editing assistance, and members of the L.A.-A. and E.G. groups for helpful discussions.

## REFERENCES

- (1) Knowles, T. P. J.; Vendruscolo, M.; Dobson, C. M. The Amyloid State and its Association with Protein Misfolding Diseases. *Nat. Rev. Mol. Cell Biol.* **2014**, *15*, 384–396.
- (2) Eisenberg, D.; Jucker, M. The Amyloid State of Proteins in Human Diseases. *Cell* **2012**, *148*, 1188–1203.
- (3) Aguzzi, A.; O'Connor, T. Protein Aggregation Diseases: Pathogenicity and Therapeutic Perspectives. *Nat. Rev. Drug Discovery* **2010**, *9*, 237–248.
- (4) Gazit, E. A Possible Role for  $\pi$ -stacking in the Self-assembly of Amyloid Fibrils. *FASEB J.* **2002**, *16*, 77–83.
- (5) McKoy, A. F.; Chen, J.; Schubach, T.; Hecht, M. H. A Novel Inhibitor of Amyloid  $\beta$  (A $\beta$ ) Peptide Aggregation: From High Throughput Screening to Efficacy in an Animal Model of Alzheimer Disease. *J. Biol. Chem.* **2012**, *287*, 38992–39000.
- (6) Makin, O. S.; Serpell, L. C. Structures for Amyloid Fibrils. *FEBS J.* **2005**, *272*, 5950–5961.
- (7) Kim, W.; Kim, Y.; Min, J.; Kim, D. J.; Chang, Y.-T.; Hecht, M. H. A High-Throughput Screen for Compounds That Inhibit Aggregation of the Alzheimer's Peptide. *ACS Chem. Biol.* **2006**, *1*, 461–469.
- (8) Roberts, B. E.; Shorter, J. Escaping Amyloid Fate. *Nat. Struct. Mol. Biol.* **2008**, *15*, 544–546.
- (9) Ono, K.; Yoshiike, Y.; Takashima, A.; Hasegawa, K.; Naiki, H.; Yamada, M. Potent Anti-Amyloidogenic and Fibril-Destabilizing Effects of Polyphenols *in Vitro*: Implications for the Prevention and Therapeutics of Alzheimer's Disease. *J. Neurochem.* **2003**, *87*, 172–181.
- (10) Pawar, A. P.; DuBay, K. F.; Zurdo, J.; Chiti, F.; Vendruscolo, M.; Dobson, C. M. Prediction of "Aggregation-Prone" and "Aggregation-Susceptible" Regions in Proteins Associated with Neurodegenerative Diseases. *J. Mol. Biol.* **2005**, *350*, 379–392.
- (11) Aguzzi, A.; Calella, A. M. Prions: Protein Aggregation and Infectious Diseases. *Physiol. Rev.* **2009**, *89*, 1105–1152.
- (12) Kapurniotu, A. Shedding Light on Alzheimer's  $\beta$ -Amyloid Aggregation with Chemical Tools. *ChemBioChem* **2012**, *13*, 27–29.
- (13) Jin, M.; Shepardson, N.; Yang, T.; Chen, G.; Walsh, D.; Selkoe, D. J. Soluble Amyloid  $\beta$ -Protein Dimers Isolated from Alzheimer Cortex Directly Induce Tau Hyperphosphorylation and Neuritic Degeneration. *Proc. Natl. Acad. Sci. U. S. A.* **2011**, *108*, 5819–5824.
- (14) Shankar, G. M.; Li, S.; Mehta, T. H.; Garcia-Munoz, A.; Shepardson, N. E.; Smith, I.; Brett, F. M.; Farrell, M. A.; Rowan, M. J.; Lemere, C. A.; Regan, C. M.; Walsh, D. M.; Sabatini, B. L.; Selkoe, D. J. Amyloid- $\beta$  Protein Dimers Isolated Directly from Alzheimer's Brains Impair Synaptic Plasticity and Memory. *Nat. Med.* **2008**, *14*, 837–842.
- (15) Bieschke, J.; Russ, J.; Friedrich, R. P.; Ehrnhoefer, D. E.; Wobst, H.; Neugebauer, K.; Wanker, E. E. EGCG Remodels Mature  $\alpha$ -Synuclein and Amyloid- $\beta$  Fibrils and Reduces Cellular Toxicity. *Proc. Natl. Acad. Sci. U. S. A.* **2010**, *107*, 7710–7715.
- (16) Porat, Y.; Abramowitz, A.; Gazit, E. Inhibition of Amyloid Fibril Formation by Polyphenols: Structural Similarity and Aromatic Interactions as a Common Inhibition Mechanism. *Chem. Biol. Drug Des.* **2006**, *67*, 27–37.

- (17) Shoval, H.; Lichtenberg, D.; Gazit, E. The Molecular Mechanisms of the Anti-amyloid Effects of Phenols. *Amyloid* **2007**, *14*, 73–87.
- (18) Ono, K.; Hasegawa, K.; Naiki, H.; Yamada, M. Curcumin has Potent Anti-amyloidogenic Effects for Alzheimer's  $\beta$ -amyloid Fibrils *in vitro*. *J. Neurosci. Res.* **2004**, *75*, 742–750.
- (19) Lakshmanan, A.; Cheong, D. W.; Accardo, A.; Fabrizio, E. D.; Hauser, C. A. E. Aliphatic Peptides Show Similar Self-assembly to Amyloid Core Sequences, Challenging the Importance of Aromatic Interactions in Amyloidosis. *Proc. Natl. Acad. Sci. U. S. A.* **2013**, *110*, 519–524.
- (20) Senguen, F. T.; Doran, T. M.; Lee, N. R.; Anderson, E. A.; Gu, X.; Ryan, D. M.; Nilsson, B. L. Probing Aromatic, Hydrophobic, and Steric Effects on the Self-assembly of an Amyloid- $\beta$  Fragment Peptide. *Mol. BioSyst.* **2011**, *7*, 486–496.
- (21) Cukalevski, R.; Boland, B.; Frohm, B.; Thulin, E.; Walsh, D.; Linse, S. Role of Aromatic Side Chains in Amyloid  $\beta$ -Protein Aggregation. *ACS Chem. Neurosci.* **2012**, *3*, 1008–1016.
- (22) Saunders, J. C.; Young, L. M.; Mahood, R. A.; Jackson, M. P.; Reville, C. H.; Foster, R. J.; Smith, D. A.; Ashcroft, A. E.; Brockwell, D. J.; Radford, S. E. An *in Vivo* Platform for Identifying Inhibitors of Protein Aggregation. *Nat. Chem. Biol.* **2016**, *12*, 94–101.
- (23) Meng, F.; Marek, P.; Potter, K. J.; Verchere, C. B.; Raleigh, D. P. Rifampicin Does Not Prevent Amyloid Fibril Formation by Human Islet Amyloid Polypeptide but Does Inhibit Fibril Thioflavin-T Interactions: Implications For Mechanistic Studies of  $\beta$ -Cell Death. *Biochemistry* **2008**, *47*, 6016–6024.
- (24) Teplow, D. B. Preparation of Amyloid  $\beta$ -Protein for Structural and Functional Studies. *Methods Enzymol.* **2006**, *413*, 20–33.
- (25) Frydman-Marom, A.; Rechter, M.; Shefler, I.; Bram, Y.; Shalev, D. E.; Gazit, E. Cognitive-Performance Recovery of Alzheimer's Disease Model Mice by Modulation of Early Soluble Amyloid Assemblies. *Angew. Chem., Int. Ed.* **2009**, *48*, 1981–1986.
- (26) Gilead, S.; Wolfenson, H.; Gazit, E. Molecular Mapping of the Recognition Interface Between the Islet Amyloid Polypeptide and Insulin. *Angew. Chem., Int. Ed.* **2006**, *45*, 6476–6480.
- (27) Shaham-Niv, S.; Adler-Abramovich, L.; Schnaider, L.; Gazit, E. Extension of the Generic Amyloid Hypothesis to Nonproteinaceous Metabolite Assemblies. *Sci. Adv.* **2015**, *1*, e150013710.1126/sciadv.1500137.
- (28) Adler-Abramovich, L.; Vaks, L.; Carny, O.; Trudler, D.; Magno, A.; Cafilisch, A.; Frenkel, D.; Gazit, E. Phenylalanine Assembly into Toxic Fibrils Suggests Amyloid Etiology in Phenylketonuria. *Nat. Chem. Biol.* **2012**, *8*, 701–706.
- (29) Reches, M.; Porat, Y.; Gazit, E. Amyloid Fibril Formation by Pentapeptide and Tetrapeptide Fragments of Human Calcitonin. *J. Biol. Chem.* **2002**, *277*, 35475–35480.
- (30) Reches, M.; Gazit, E. Casting Metal Nanowires Within Discrete Self-assembled Peptide Nanotubes. *Science* **2003**, *300*, 625–627.
- (31) Reches, M.; Gazit, E. Self-assembly of Peptide Nanotubes and Amyloid-like Structures by Charged-termini-capped Diphenylalanine Peptide Analogues. *Isr. J. Chem.* **2005**, *45*, 363–371.
- (32) Kim, W.; Hecht, M. H. Generic Hydrophobic Residues are Sufficient to Promote Aggregation of the Alzheimer's A $\beta$ 42 Peptide. *Proc. Natl. Acad. Sci. U. S. A.* **2006**, *103*, 15824–15829.
- (33) Grabowski, T. J.; Cho, H. S.; Vonsattel, J. P. G.; Novel Amyloid Precursor Protein Mutation in an Iowa Family with Dementia and Severe Cerebral Amyloid Angiopathy *Ann. Neurol.* **2001**, *49*, 697–705.10.1002/ana.1009.
- (34) Scherzer-Attali, R.; Pellarin, R.; Convertino, M.; Frydman-Marom, A.; Egoz-Matia, N.; Peled, S.; Levy-Sakin, M.; Shalev, D. E.; Cafilisch, A.; Gazit, E.; Segal, D. Complete Phenotypic Recovery of an Alzheimer's Disease Model by a Quinone-Tryptophan Hybrid Aggregation Inhibitor. *PLoS One* **2010**, *5*, e11101.
- (35) Souza, M. I.; Silva, E. R.; Jaques, Y. M.; Ferreira, F. F.; Fileti, E. E.; Alves, W. A. The Role of Water and Structure on the Generation of Reactive Oxygen Species in Peptide/Hypericin Complexes. *J. Pept. Sci.* **2014**, *20*, 554–562.
- (36) Shoval, H.; Weiner, L.; Gazit, E.; Levy, M.; Pinchuk, I.; Lichtenberg, D. Polyphenol-Induced Dissociation of Various Amyloid Fibrils Results in a Methionine-Independent Formation of ROS. *Biochim. Biophys. Acta, Proteins Proteomics* **2008**, *1784*, 1570–1577.
- (37) Amdursky, N.; Molotskii, M.; Aronov, D.; Adler-Abramovich, L.; Gazit, E.; Rosenman, G. Blue Luminescence Based on Quantum Confinement at Peptide Nanotubes. *Nano Lett.* **2009**, *9*, 3111–3115.
- (38) Pinotsi, D.; Buell, A. K.; Dobson, C. M.; Kaminski Schierle, G. S.; Kaminski, C. F. A Label-Free, Quantitative Assay of Amyloid Fibril Growth Based on Intrinsic Fluorescence. *ChemBioChem* **2013**, *14*, 846–850.
- (39) Esbjörner, E. K.; Chan, F.; Rees, E.; Erdelyi, M.; Luheshi, L. M.; Bertocini, C. W.; Kaminski, C. F.; Dobson, C. M.; Kaminski Schierle, G. S. Direct Observations of Amyloid  $\beta$  Self-Assembly in Live Cells Provide Insights into Differences in the Kinetics of A $\beta$ (1–40) and A $\beta$ (1–42) Aggregation. *Chem. Biol.* **2014**, *21*, 732–742.10.1016/j.chembiol.2014.03.014.
- (40) Knowles, T. P. J.; Buehler, M. J. Nanomechanics of Functional and Pathological Amyloid Materials. *Nat. Nanotechnol.* **2011**, *6*, 469–479.
- (41) Kol, N.; Adler-Abramovich, L.; Barlam, D.; Shneck, R. Z.; Gazit, E.; Rousso, I. Self-Assembled Peptide Nanotubes Are Uniquely Rigid Bioinspired Supramolecular Structures. *Nano Lett.* **2005**, *5*, 1343–1346.
- (42) Azuri, I.; Adler-Abramovich, L.; Gazit, E.; Hod, O.; Kronik, L. Why are Diphenylalanine-based Peptide Nanostructures So Rigid? Insights from First Principles Calculations. *J. Am. Chem. Soc.* **2014**, *136*, 963–969.
- (43) Lutticke, C.; Hauske, P.; Lewandrowski, U.; Sickmann, A.; Kaiser, M.; Ehrmann, M. E. coli LoIP (YggG), a Metalloprotease Hydrolyzing Phe–Phe Bonds. *Mol. BioSyst.* **2012**, *8*, 1775–1782.
- (44) Niu, L.; Liu, L.; Xi, W.; Han, Q.; Li, Q.; Yu, Y.; Huang, Q.; Qu, F.; Xu, M.; Li, Y.; Du, H.; Yang, R.; Cramer, J.; Gothelf, K. V.; Dong, M.; Besenbacher, F.; Zeng, Q.; Wang, C.; Wei, G.; Yang, Y. Synergistic Inhibitory Effect of Peptide-Organic Coassemblies on Amyloid Aggregation. *ACS Nano* **2016**, *10*, 4143–4153.
- (45) Soto, C.; Sigurdsson, E. M.; Morelli, L.; Kumar, R. A.; Castaño, E. M.; Frangione, B.  $\beta$ -Sheet Breaker Peptides Inhibit Fibrillogenesis in a Rat Brain Model of Amyloidosis: Implications for Alzheimer's Therapy. *Nat. Med.* **1998**, *4*, 822–826.
- (46) Lin, L. X.; Bo, X. Y.; Tan, Y. Z.; Sun, F. X.; Song, M.; Zhao, J.; Ma, Z. H.; Li, M.; Zheng, K. J.; Xu, S. M. Feasibility of  $\beta$ -sheet Breaker Peptide-H102 treatment for Alzheimer's Disease Based on  $\beta$ -amyloid Hypothesis. *PLoS One* **2014**, *9* (11), e112052.
- (47) Kaffy, J.; Brinet, D.; Soulier, J. L.; Khemtémourian, L.; Lequin, O.; Taverna, M.; Crousse, B.; Ongeri, S. Structure-activity Relationships of Sugar-based Peptidomimetics as Modulators of Amyloid  $\beta$ -peptide Early Oligomerization and Fibrillization. *Eur. J. Med. Chem.* **2014**, *86*, 752–758.
- (48) Scherzer-Attali, R.; Shaltiel-Karyo, R.; Adalist, Y. H.; Segal, D.; Gazit, E. Generic Inhibition of Amyloidogenic Proteins by Two Naphthoquinone–Tryptophan Hybrid Molecules. *Proteins: Struct., Funct., Genet.* **2012**, *80*, 1962–1973.
- (49) Iuvone, T.; De Filippis, D.; Esposito, G.; D'Amico, A.; Izzo, A. A. The Spice Sage and its Active Ingredient Rosmarinic Acid Protect PC12 Cells from Amyloid- $\beta$  Peptide-Induced Neurotoxicity. *J. Pharmacol. Exp. Ther.* **2006**, *317*, 1143–1149.
- (50) Alkam, T.; Nitta, A.; Mizoguchi, H.; Itoh, A.; Nabeshima, T. A Natural Scavenger of Peroxynitrites, Rosmarinic Acid, Protects Against Impairment of Memory Induced by A $\beta$ 25–35. *Behav. Brain Res.* **2007**, *180*, 139–145.
- (51) Ono, K.; Hasegawa, K.; Yoshiike, Y.; Takashima, A.; Yamada, M.; Naiki, H. Nordihydroguaiaretic Acid Potently Breaks down Pre-Formed Alzheimer's Beta-Amyloid Fibrils *in Vitro*. *J. Neurochem.* **2002**, *81*, 434–440.
- (52) Goodman, Y.; Steiner, M. R.; Steiner, S. M.; Mattson, M. P. Nordihydroguaiaretic Acid Protects Hippocampal Neurons Against Amyloid  $\beta$ -peptide Toxicity, and Attenuates Free Radical and Calcium Accumulation. *Brain Res.* **1994**, *654*, 171–176.

(53) Diomede, L.; Cassata, G.; Fiordaliso, F.; Salio, M.; Ami, D.; Nataello, A.; Doglia, S. M.; De Luigi, A.; Salmona, M. Tetracycline and Its Analogues Protect *Caenorhabditis Elegans* from  $\beta$  Amyloid-Induced Toxicity by Targeting Oligomers. *Neurobiol. Dis.* **2010**, *40*, 424–431.

(54) Forloni, G.; Colombo, L.; Girola, L.; Tagliavini, F.; Salmona, M. Anti-amyloidogenic Activity of Tetracyclines: Studies *in vitro*. *FEBS Lett.* **2001**, *487*, 404–407.

(55) Ehrnhoefer, D. E.; Bieschke, J.; Boeddrich, A.; Herbst, M.; Masino, L.; Lurz, R.; Engemann, S.; Pastore, A.; Wanker, E. E. EGCG Redirects Amyloidogenic Polypeptides into Unstructured, off-Pathway Oligomers. *Nat. Struct. Mol. Biol.* **2008**, *15*, 558–566.

(56) Young, L. M.; Saunders, J. C.; Mahood, R. A.; Revill, C. H.; Foster, R. J.; Tu, L.-H.; Raleigh, D. P.; Radford, S. E.; Ashcroft, A. E. Screening and Classifying Small-Molecule Inhibitors of Amyloid Formation Using Ion Mobility Spectrometry–mass Spectrometry. *Nat. Chem.* **2015**, *7*, 73–81.

(57) Arnon, Z. A.; Vitalis, A.; Levin, A.; Michaels, T. C. T.; Caflish, A.; Knowles, T. P. J.; Adler-Abramovich, L.; Gazit, E. Dynamic Microfluidic Control of Supramolecular Peptide Self-Assembly. *Nat. Commun.* **2016**, *7*, 13190.

(58) Mason, T. O.; Chirgadze, D. Y.; Levin, A.; Adler-Abramovich, L.; Gazit, E.; Knowles, T. P. J.; Buell, A. K. Expanding the Solvent Chemical Space for Self-Assembly of Dipeptide Nanostructures. *ACS Nano* **2014**, *8*, 1243–1253.

(59) Lanucara, F.; Holman, S. W.; Gray, C. J.; Eyers, C. E. The Power of Ion Mobility-Mass Spectrometry for Structural Characterization and the Study of Conformational Dynamics. *Nat. Chem.* **2014**, *6*, 281–294.

(60) Mehmood, S.; Allison, T. M.; Robinson, C. V. Mass Spectrometry of Protein Complexes: From Origins to Applications. *Annu. Rev. Phys. Chem.* **2015**, *66*, 453–474.

(61) Do, T. D.; De Almeida, N. E. C.; LaPointe, N. E.; Chamas, A.; Feinstein, S. C.; Bowers, M. T. Amino Acid Metaclusters: Implications of Growth Trends on Peptide Self-Assembly and Structure. *Anal. Chem.* **2016**, *88*, 868–876.